

Original Article

The traditional Chinese medicine infradiaphragmatic stasis-expelling decoction (ISED) is effective in the alleviation of NAFLD in rats

Jie Ma, Anhua Shi, Wenhui Chen

College of Pre-clinical Medicine, Yunnan University of Chinese Medicine, Kunming 650000, Yunnan, People's Republic of China

Received August 2, 2017; Accepted January 11, 2019; Epub May 15, 2019; Published May 30, 2019

Abstract: The traditional Chinese medicine Infradiaphragmatic Stasis-Expelling Decoction (ISED) has been utilized to alleviate the symptoms of non-alcoholic fatty liver disease (NAFLD) in China. However, the specific mechanism involved has still not been explored. The aim of the paper is to investigate the effects of ISED on NAFLD rats and reveal the potential mechanism. One-hundred rats were divided into model and control groups. The animals in the model group were fed a high fat diet (HFD) for 8 weeks to establish the NAFLD model. The control animals were fed an ordinary diet. Twenty-five animals in the model group were selected as the ISED group at the beginning of the 9th week, and intragastrically administrated ISED (30 mg/kg.d) through the end of the 12th week. Ten rats in each group were sacrificed to collect liver tissues and blood at the end of the 10th and 12th weeks. The results showed that ISED significantly reduced the body weight, wet liver weight, and hepatosomatic index of the NAFLD rats. The ALT and AST activities, as well as the TC and TG contents in the serum in ISED group, were significantly lower than those in the model group. A lower steatosis level and fewer fatty areas in the liver tissues in the ISED group were observed compared to the model group. The microstructure of the liver tissues and cells in the ISED group was less damaged than the microstructure in the model group. A hemorheology assay showed that ISED administration decreased the platelet aggregation ratio and whole blood viscosity of the NAFLD rats as indicated by the reduction of the vWF, GPIIb/IIIa, fibrinogen, and CD62p contents in the serum. Taken together, our data suggest that ISED is effective in improving the symptoms of NAFLD in rats.

Keywords: Traditional Chinese medicine, infradiaphragmatic stasis-expelling decoction, non-alcoholic fatty liver disease, rats

Introduction

Non-alcoholic fatty liver disease (NAFLD) has become the most common liver disease in China, with the rapid improvement of living conditions [1]. In Western countries, NAFLD is the second most common cause for liver transplants and the most common cause of hepatocellular carcinoma (HCC) [2, 3]. NAFLD can deteriorate into fatty hepatitis, hepatic fibrosis, and liver cancer, leading to the risk of mortality unless it was well controlled and treated [4, 5]. NAFLD is also notorious for its high frequency of causing complications of diabetes and cardiac diseases [6, 7].

Due to the limited understanding to the pathogenesis of NAFLD, no modern drugs have been

authorized by the FDA for the treatment of NAFLD, although several compounds are undergoing clinical trials [8]. Traditional Chinese medicine (TCM) has achieved a rich experience in the treatment of NAFLD [9-11]. The therapeutic scheme of TCM treatment completely differs from those of Western medicines in European and American countries (as with Western medicine in China). The treatment with Western medicines usually utilizes one chemically synthesized structure directed at a specific target to treat a certain disease. In TCM treatment, the doctors will prescribe a mixture of several kinds of herbal medicines, in which the diversity of natural compounds are synergistically responsible for the treatment by simultaneously directing several compounds at unknown targets [12]. Although the period of TCM treatment

Infradiaphragmatic stasis-expelling decoction

is typically longer than the treatment period in Western medicine, the patients are more favorable to TCM, especially in the treatment of chronic disease in China, because recovered patients who underwent TCM treatment are not easily subjected to the recurrence of illness [13].

Infradiaphragmatic stasis-expelling decoction (ISED) was originally recorded in *Corrections on the Errors of Medical Works* created by Qingren Wang in the Qing Dynasty. ISED is a compound recipe, which is made of 12 herbal medicines including *Angelica sinensis*, *Ligusticum chuanxiong*, *Prunus persica*, *Paeonia veitchii*, *Faeces trogopterori*, *Lindera aggregata*, *Corydalis turtschaninovii*, *Cyperus rotundus*, *Carthamus tinctorius*, *Citrus aurantium*, *Glycyrrhiza uralensis*, and *Aeonium suffruticosum* [14]. ISED was popularly used in the treatment of hepatitis, early liver cirrhosis, colitis gravis, NAFLD, and tuberculous peritonitis in China [15, 16]. The core ideal of ISED in treating disease has been thought to be its ability to accelerate blood circulation and dissolve stasis, followed by an improvement of hypercoagulation and thrombophilia. Apart from a decrease of fat in the blood and liver tissues, the improvement of hypercoagulation and thrombophilia is regarded to be one of the key strategies for the treatment of NAFLD in TCM [17]. However, the hypothesis has been not proved *in vitro*. Therefore, we have duplicated the NAFLD rat model by using the HFD induction. And the NAFLD rats were intervened using the ISED complication to reveal the effect and potential mechanisms of ISED on NAFLD.

Materials and methods

Preparation of ISED

Angelica sinensis (11 g), *Ligusticum chuanxiong* (21 g), *Prunus persica* (11 g), *Paeonia veitchii* (45 g), *Faeces trogopterori* (18 g), *Lindera aggregata* (78 g), *Corydalis turtschaninovii* (23 g), *Cyperus rotundus* (7 g), *Carthamus tinctorius* (128 g), *Citrus aurantium* (4 g), *Glycyrrhiza uralensis* (25 g), and *Aeonium suffruticosum* (7 g) were boiled in 2000 mL water. After 3 h of heat, the extract was cooled and concentrated under reduced pressure to get a crude extract (0.98 g/cm³), which was stored in the refrigerator at 4°C.

Animals and groups

One-hundred rats were purchased from the Animal Center of Kunming Medical University (ACKMU). The animals were housed at a constant temperature (20-25°C), humidity (40-70%) and light-dark cycle (12/12 h) in the animal center of Yunnan University of Chinese Medicine. The experiments began after an acclimation period of one week. The rats were randomly divided into a model group (n=50) and a control group (n=50). The rats in the control group were fed ordinary feed, while the rats in the model group were fed a high fat diet (HFD, 88% ordinary feed, 10% lard, and 2% cholesterol). After 8-weeks of feeding, twenty five rats in the model group were selected as the ISED group which was intragastrically given ISED (30 mg/kg.d, at 9:00 a.m, one administration per day). The remaining twenty five animals in the model group were intragastrically given the same dosage of normal saline. The treatment was continued through the end of the 12th week. During the treatment, the animals in the ISED and model groups were fed HFD, and the animals in the control group were given ordinary feed. After 10 and 12 weeks, ten rats in each group were sacrificed. Their liver tissues and blood were collected for the biological and histopathological assays. All the experiments were conducted under the National Institute of Health's *Guide for the Care and Use of Laboratory Animals* and approved by the Ethics Committee (Animal Care and Use Committee) of Yunnan University of Chinese Medicine. All efforts were made to minimize the pain and suffering of the animals.

General morphological observation

The body weight (BW), wet liver weight (WLW), and hepatosomatic index (HI) were obtained from each rat and calculated using the standard assay.

Preparation of serum and liver tissue

The serum samples were prepared following the blood clotting. Blood samples were allowed to clot at 4°C and centrifuged at 5,000 g for 10 min before harvesting the serum. The serum samples were then stored at -20°C for the following assay. The livers were stripped and fixed in 10% formalin at 4°C for the assay. Another

part of the aorta and the liver was immediately placed in the 10 mL dorf tube containing 0.1% diethyl pyrocarbonate water. Then the samples were autoclaved and thereafter stored at -80°C for the assay.

Biochemical assay

Triglyceride (TG) and total cholesterol (TC) contents in the serum and liver tissues were determined using a Clean Tech TG-S Kit (3I1570; Asanpharm, Hwaseong, Korea) and a T-CHO Kit (3I2020; Asanpharm, Hwaseong, Korea) following the manufacturer's instructions. The total protein content was determined using the BCA method (Sigma). The activities of alanine transaminase (ALT) and aspartate transaminase (AST) were assessed by a kinetic method with the use of dedicated diagnostic kits (bioMerieux and Pointe Scientific Inc). Fibrinogen (Fib) was estimated by the nephelometric method after heat precipitation in buffered saline. Glycoprotein IIb/IIIa (GP IIb/IIIa) contents were assayed using flow cytometry (BD Bioscience, USA). The concentration of von Willebrand factor (VWF) was determined using a standard enzyme-linked immunoabsorbent assay (ELISA). VWF was captured using a monoclonal antibody, AVW-1, and detected using a rabbit anti-human VWF polyclonal antibody. Levels of CD62p (p-selectin) were determined using a commercial ELISA kit from R&D Systems (Abingdon, Oxon, United Kingdom) as described previously [10]. Arterial blood was citrated using 3.28% sodium citrate (1:9, v/v) and then centrifuged at 1020 g to obtain the platelet-rich plasma (PRP).

Hemorheology assay

The platelet aggregation ratio (PAR) was measured by a platelet aggregation analyzer (DX-800, Beckmann, USA). The calculation of red blood cells (RBC) was carried out using a blood cell counter (Orphee mythic 22, Switzerland). Blood viscosity measurements were made on venous blood samples at multiple shear rates using an automatic tube viscometer (RheologTM, Health Vector Co., Pennsauken, NJ) operating at 37°C . In brief, the device uses a horizontal glass tube (~ 0.8 mm ID) that has vertical fluid manometers at each end. The blood sample is introduced in such a way that there is initially a pressure gradient (i.e., difference in height of blood in manometers), and then it is allowed to flow through the tube. The pressure gradient

progressively decreases as the heights tend to equalize. The positions of the blood in each manometer are continuously recorded, thus providing a pressure gradient and volumetric flow information as a function of time. The pressure-flow data are analyzed by computer software provided by the manufacturer to obtain apparent blood viscosity versus shear rate results. Low shear viscosity (LSV), moderate shear viscosity (MSV), and high shear viscosity (HSV) are reported at pre-selected shear rates from 1 to 50 s^{-1} , 5 to 100 s^{-1} , and 10 to 1000 s^{-1} , respectively. The ratio of whole blood viscosity (WBV) was selected at 5 to 300 s^{-1} .

Quantitative real-time (RT) PCR

Total RNA was isolated using Trizol (Invitrogen, Carlsbad, CA, USA) according to the manufacturer's instructions. QRT-PCR was conducted to assess the expression level of using the $2^{-\Delta\Delta\text{CT}}$ method. β -actin was used as an internal standard to normalize the expression level.

HE staining

The liver samples were fixed in PBS containing 4% paraformaldehyde. After they were deparaffinized in xylene and rehydrated in 85% ethanol, the slides were stained with hematoxylin (2 min) and then cleaned by distilled water and 70% ethanol (containing 0.1% hydrochloric acid). Next, the slides were stained with 0.5% eosin for 2 min and rinsed again with distilled water. Finally, the slides were dehydrated with 95% and 100% ethanol successively, followed by xylene (3 min) and mounted with coverslips.

Oil red O staining

A portion of the liver tissues was fixed with 10% formalin and embedded in paraffin. 10-micron thick sections were cut and stained with oil red O for the examination of adipose tissue histology (IX-81, Olympus Corporation, Tokyo, Japan). The adipocyte cross-sectional area was measured using an ImageJ 1.43 analyzing system.

Electron microscopy

The ultrastructure of LSEC (liver sinusoidal endothelial cells) was observed using a transmission electron microscope. The specimens were fixed in 2% glutaraldehyde in a 0.1 M phosphate buffer (pH=7.4) for 4 h and washed in a phosphate buffer 0.1 M (pH=7.4) for 4×30 min. The specimens were post-fixed in 2% osmi-

um tetroxide in 0.1 M phosphate buffer (pH=7.4) for 4 h, washed and then dehydrated in a graded series of alcohols. The specimens were embedded in Spurr's resin and thin sections were cut. Between 2 and 4 levels of 4 blocks in each sample were examined at magnifications of 12,000× using a Philips CM 10 transmission electron microscope (Royal Philips Electronics, Holland). Approximately 30 sinuoids from each animal were assessed.

Statistical analysis

Student's *t* test or one-way ANOVA were used for the statistical analysis when appropriate. All statistical analyses were performed using SPSS 19.0 (SPSS Inc., Chicago, IL, USA). A value of $P < 0.05$ was considered statistically significant.

Results

ISED reduced the BW, WLW, and HI of NAFLD rats

As shown in **Table 1**, the BW of animals in the model group was not significantly different from the BW in the control and ISED groups at the end of the 10th week. However, BW in the model group at the end of the 12th week was significantly higher than the BW in the control and ISED groups. The average BW of rats in the ISED group was the lowest, and was not statistically different from the BW of the animals in the control group at the end of the 10th and 12th weeks. The administration of ISED lowered the BW increase induced by the HFD. The WLW in the ISED and control groups was not significantly different at the end of both the 10th and 12th weeks. The WLW in the model group was significantly higher than the WLW in the control and model groups at the end of the 10th and 12th weeks. The distribution of HI was similar to that of WLW. Animals in the model group showed significantly higher HI values than those in control and ISED groups at the end of both the 10th and 12th weeks. There was no statistical differentiation in HI between the control and ISED groups at the end of the 10th and 12th weeks (**Table 1**). The above observation suggests that ISED is capable of reducing the BW, WLW, and HI values of HFD-induced NAFLD rats.

ISED reduced the TC and TG contents as well as the ALT and AST activities in the liver tissues and serum of NAFLD rats

Both the TC and TG contents in the serum of the three groups at the end of the 10th week were not significantly different from those at the end of the 12th week. The model group showed significantly higher TC and TG contents than the control and ISED groups at the end of the 10th and 12th weeks. The serum TC and TG contents in the ISED group were in-between the control and model groups at the end of both the 10th and 12th weeks. The change pattern of the TC and TG contents in the liver tissues was very similar to the pattern in the serum. The TC contents of the livers in the model group were significantly higher than those in the control and ISED groups at the end of the 10th and 12th weeks. Although there was no statistical difference in the livers' TG among the three groups, the average TG levels of the liver tissues in model group were the highest at the end of both the 10th and 12th weeks, and the control group had the lowest liver TG levels (**Table 2**). The activities of ALT and AST in the control group were not significantly different from those in the ISED group at the end of the 10th and 12th weeks. However, the activities of ALT and AST in the model group were significantly higher than those in the control and ISED groups at the end of the 10th and 12th weeks (**Table 3**). Those results indicated that ISED administration reduced the TC and TG levels as well as the ALT and AST activities in the liver tissues and the serum of the NAFLD rats.

ISED altered the hemorheology of NAFLD rats

The PAR and WBV in the ISED group were not statistically different from the PAR and WBV in the control group at the end of both the 10th and 12th weeks, and were significantly lower than those in the model group. However, there was no statistical differentiation in the RBC between the three groups at the end of both the 10th and 12th weeks (**Table 4**). The LSV, MSV, and HSV in the control group were significantly lower than they were in the model group at the end of the 10th and 12th weeks. The LSV and MSV in the ISED group at the end of the 10th and 12th weeks were significantly lower than they were in the model group except the

Infradiaphragmatic stasis-expelling decoction

Table 1. The effects of ISED on BW (g), WLF (%) and HI in NAFLD rats

Groups	10 th weekend			12 th weekend		
	BW	WLW	HI	BW	WLW	HI
Control	399.8±26.8	9.7±0.8	3.9±0.3	428.8±19.9	9.5±0.5	4.4±0.2
Model	414.8±41.8	13.6±1.1*	9.7±0.8	498.2±21.8* ^{#,Δ}	13.5±1.4* [#]	5.2±2.1* [#]
ISED	388.2±22.8	11.4±0.9	3.7±0.3	414.6±31.2	10.7±1.0*	3.9±0.5

BW: body weight; WIW: wet liver weight; HI: hepatosomatic index. *P<0.01 vs control; #P<0.05 vs ISED; ΔP<0.05 vs 10th weekend.

Table 2. The effects of ISED on the contents of TC (mmol/L) and TG (mmol/L) in NAFLD rats

Tissues	Groups	10 th weekend		12 th weekend	
		TC	TG	TC	TG
Serum	Control	1.7±0.1	0.71±0.03	1.72±0.23	0.68±0.35
	Model	2.4±0.0* ^{#,*}	1.1±0.02	2.30±0.29* [#]	1.36±0.26* [#]
	ISED	2.0±0.1*	0.99±0.05*	2.05±0.31*	1.01±0.27*
Livers	Control	2.5±0.2	0.34±0.05	2.30±0.32	0.30±0.07
	Model	6.9±0.5* [#]	0.36±0.09	8.80±0.52* ^{#,Δ}	0.38±0.10
	ISED	3.2±0.2*	0.35±0.06	3.73±0.23*	0.34±0.07

TC: total cholesterol; TG: Triglyceride. *P<0.05 vs control; #P<0.05 vs ISED; ΔP<0.05 vs 10th weekend.

Table 3. Effect of ISED on the activities of ALT (U/L) and AST (U/L) in NAFLD rats

Groups	10 th weekend		12 th weekend	
	ALT	AST	ALT	AST
Control	25.4±1.8	17.6±1.1	25.5±1.0	18.9±1.0
Model	48.4±2.0* [#]	54.3±1.5* [#]	51.6±5.6* [#]	61.2±5.9* ^{#,Δ}
ISED	36.4±1.4*	19.8±0.5	35.4±3.2*	17.6±0.2 ^Δ

ALT: alanine transaminase; AST: aspartate transaminase. *P<0.05 vs Control; #P<0.05 vs ISED; ΔP<0.05 vs 10 weekend.

HSV, which was not statistically different from the HSV in the model group (**Table 5**). Except for RBC and HSV, the above hemorheology parameters in the NAFLD rats were altered due to the ISED administration.

ISED reduced the contents of Fib, vWF, GPIIb/IIIa, and CD62p in the serum of NAFLD rats

The contents of four main cytokines (Fib, vWF, GPIIb/IIIa, and CD62p), which were associated with the hemorheology, were measured. As shown in **Table 6**, the control group had lower Fib levels at the end of the 10th week than the model and ISED groups. The fib contents in the model group were significantly higher than those in the ISED group at the end of the 10th week. The contents of Fib in the model and control became higher at the end of the 12th week

than they were at the end of the 10th week. However, the Fib contents in the ISED group at the end of the 12th week were more decreased than they were at the end of the 10th week, which was significantly lower than they were in model group. The CD62p contents in the control were significantly lower than in the model group at the end of the 10th and 12th weeks. After oral administration of ISED, the CD62p contents in the ISED group were significantly lower than those in model group at the end of both the 10th and 12th weeks (**Table 6**). The transformation of vWF and GPIIb/IIIa was similar to that of Fib and CD62p. The highest contents of vWF and

GPIIb/IIIa were found in the model group at the end of the 10th and 12th weeks and the control group showed the lowest contents of vWF and GPIIb/IIIa. After oral administration of ISED, the contents of vWF and GPIIb/IIIa in the ISED group were significantly lower than those in the model group at the end of the 10th and 12th weeks (**Table 6**).

ISED regulated the m-RNA levels of Fib and CD62p

The results of RT PCR showed that the m-RNA levels of the four cell factors in the model group were higher than those in the control, indicating that the four cell factors were up-regulated by HFD (**Figure 1**). The ISED animals showed that the m-RNA levels of Fib and CD62p were parallel to the control animals at the end of both the

Infradiaphragmatic stasis-expelling decoction

Table 4. Effect of ISED on PAR (%), WBV (mPa.S), and RBC (10^9 /mL) in NAFLD rats

Group	10 th weekend			12 th weekend		
	PAR	WBV	RBC	PAR	WBV	RBC
Control	7.78±0.85	9.55±3.09	3.98±0.13	8.29±0.63	9.17±2.08	4.02±0.54
Model	8.65±0.53 ^{*,#}	14.79±3.95 ^{*,#}	3.95±0.19	9.47±1.04 ^{*,#,\Delta}	13.63±4.46 ^{*,#}	3.87±0.41
ISED	7.77±0.36	9.13±2.47	4.04±0.30	8.46±0.50 ^{\Delta}	9.05±2.92	3.89±0.26

PAR: platelet aggregation ratio; WBV: whole blood viscosity; RBC: red blood cells ^{*}P<0.05 vs Control; [#]P<0.05 vs ISED; ^{\Delta}P<0.05 vs 10th weekend.

Table 5. Effect of ISED on LSV, MSV, and HSV (mPa.S) in NAFLD rats

Group	10 th weekend			12 th weekend		
	LSV	MSV	HSV	LSV	MSV	HSV
Control	42.60±5.40	6.53±0.54	4.24±0.48	44.1±9.30	6.61±1.02	5.29±0.76
Model	51.20±5.78 ^{*,#}	8.03±1.36 ^{*,#}	5.48±1.24 [*]	58.40±3.36 ^{*,#}	8.98±1.18 ^{*,#}	6.38±1.02 [*]
ISED	36.23±3.14	5.76±0.38	5.35±0.29 [*]	45.54±4.94 ^{\Delta}	6.75±0.86	6.39±0.74 [*]

LSV: low shear viscosity; MSV: moderate shear viscosity; HSV: high shear viscosity. ^{*}P<0.05 vs Control; [#]P<0.05 vs ISED; ^{\Delta}P<0.05 vs 10th weekend.

Table 6. Effect of ISED on the levels of Fib (g/L), CD62p (pg/mL), vWF (pg/mL), and GPIIb/IIIa (U/mL) in the serum of NAFLD rats

Group	10 th weekend				12 th weekend			
	Fib	CD62p	vWF	GPIIb/IIIa	Fib	CD62p	vWF	GPIIb/IIIa
Control	2.6±0.2	74.5±19.3	942.0±158.0	608.3±59.8	3.0±0.3	63.7±16.7	938.0±170.0	595.2±62.4
Model	3.7±0.8 [*]	345.8±19.0 ^{*,#}	2526.2±288.8 ^{*,#}	1075.0±86.2 ^{*,#}	4.0±0.90 ^{*,#}	327.5±42.3 ^{*,#}	2638±369.1 ^{*,#}	1139.5±87.2 ^{*,#}
ISED	3.2±0.4 [*]	202.3±21.0 [*]	1934.0±216.3 [*]	580.9±66.6	2.80±0.4	202.1±24.0 [*]	1815±193.4 [*]	745.1±53.1 ^{*,\Delta}

Fib: fibrinogen; vWF: von Willebrand Factor; CD62p: P-selectin; GPIIb/IIIa: glycoprotein IIb/IIIa. ^{*}P<0.05 vs Control; [#]P<0.05 vs ISED; ^{\Delta}P<0.05 vs 10th weekend.

10th and 12th weeks. However, the m-RNA levels of vWF and GPIIb/IIIa in ISED group were not significantly different from those in the model group at the end of the 10th and 12th weeks (Figure 1).

ISED alleviated the damage of the liver micro-structure in NAFLD rats

In the control group, the structure of lobuli hepatis was normal at the end of the 10th week. The hepatic cord was arrayed fitly. The shape of the fatty cells was homogeneous, oval shaped. No invasion of inflammatory cells or fibrous tissues hyperplasia were observed in the portal areas (Figure 2). A larger number of liver cells in the model group at the end of the 10th week were turned into fatty cells, and the hepatic cord was ordered irregularly. The anthonisma of the liver cells made the hepatic cord blurry, but, there were still no inflammatory cell invasions and fibrous tissue hyperplasia was observed in the portal areas. A small percentage of liver cells was lightly steatotic, showing different

sizes of fat vacuoles in the cytoplasm in the ISED group at the end of the 10th week. Hepatic cords in the ISED group at the 10th weekend were also disordered (Figure 2). The pathological status of the live tissues in the control group at the end of the 12th week were similar to those at the end of the 10th week. No pathological change was detected in the control group at the end of the 12th week. However, almost all the liver cells were steatotic and swelling at the end of the 12th week in the model group. The array of hepatic cords at the end of the 12th week in the ISED group become more regular than it was at the end of the 10th week, but a small percentage of the liver cells were still lightly steatotic (Figure 2).

Adipocyte staining showed that the liver tissues in the control group were dyed a blurry orange at the end of both the 10th and 12th weeks, indicating a strong degree of steatosis (Figure 3). A light orange color was observed in the adipocyte staining of the livers in ISED group at both the end of the 10th and 12th weeks, suggesting

Infradiaphragmatic stasis-expelling decoction

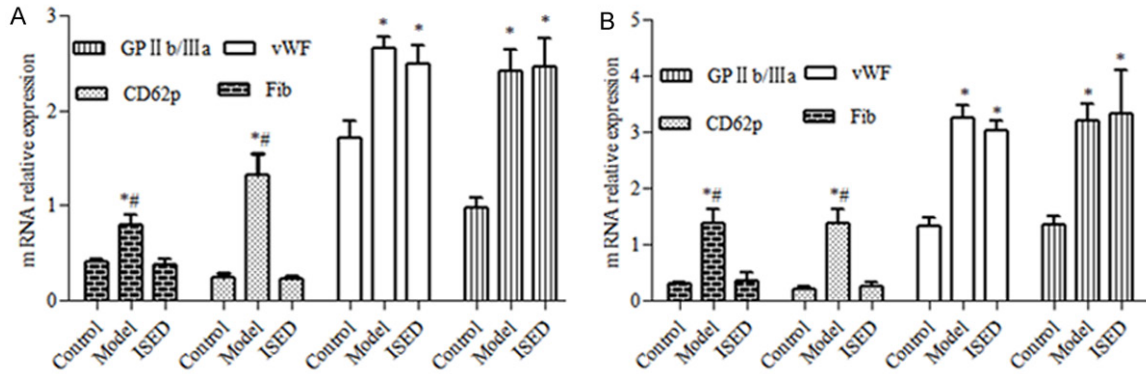


Figure 1. m-RNA levels of Fib, CD62p, vWF, and GPIIb/IIIa in the serum of NAFLD rats. (A): 10th weekend (B): 12th weekend. m-RNA expression was normalized relative to β -actin. All the experiments were repeated three times, * $P < 0.05$ vs Control, # $P < 0.05$ vs ISED.

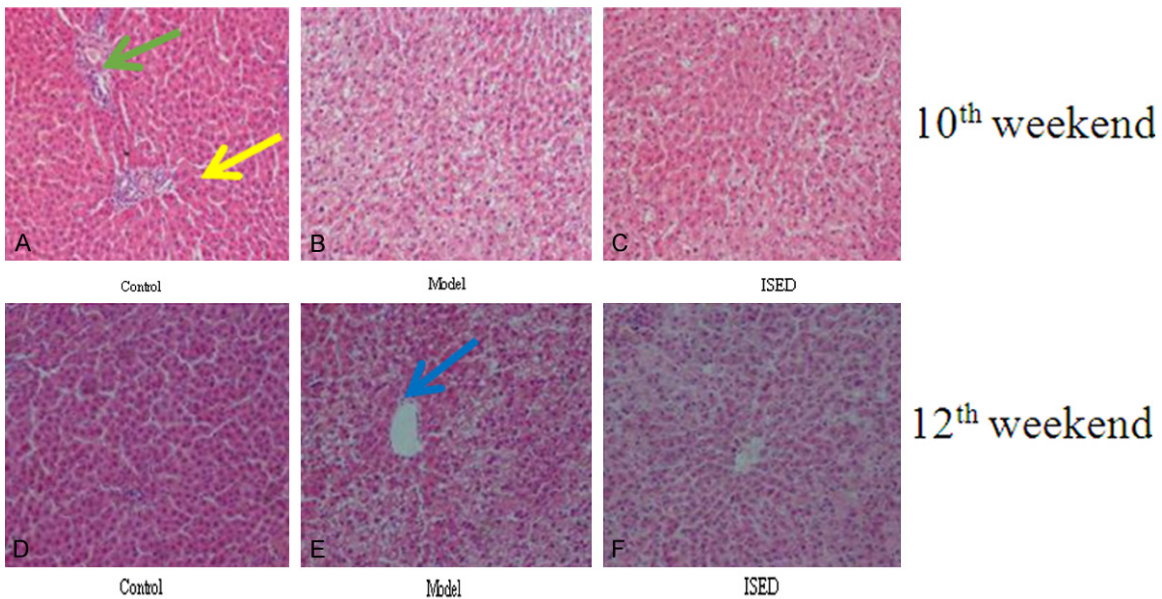


Figure 2. HE staining of liver tissue. The slide was observed using an Olympus CX-23 microscope (800 \times). Ten visual fields in a single assay were selected randomly. The structure of lobuli hepatis (green arrow), hepatic cord (yellow arrow), and the fatty cells (blue arrow) was shown. (A): Structure of lobuli hepatis was normal. Hepatic cord was fitly arrayed. (B): A larger number of liver cells were turned into fatty cells. The hepatic cord was ordered irregularly. (C): A small percentage of liver cells was lightly steatotic. Hepatic cords were disordered. (D): The structure of the lobuli hepatis was normal. The hepatic cord was fitly arrayed (E): Almost all liver cells were steatotic and swollen. (F): A small percentage of liver cells were still lightly steatotic. The array of hepatic cords become more regular than that at 10th weekend.

a low degree of steatosis. However, a middling level of liver tissue steatosis in the model group at the end of the 10th and 12th weeks was hinted at as indicated by the moderate orange in adipocyte staining. Although the fatty areas of livers in the ISED group were significantly larger than those in control group, the ISED animals showed significantly smaller fatty areas of livers than the model group at the end of the 10th and 12th week. ISED reduced the steatosis lev-

els and the fatty areas of livers in the HFD-induced NAFLD rat model.

The ultrastructure of LSEC was sound in the control and ISED groups at the end of the 10th and 12th weeks (Figure 4). But the LSEC in model group was swelling at the ends of both the 10th and 12th weeks, of which the mitochondria and endoplasmic reticulum seemed inflatable. A portion of the LSEC was hurt and frag-

Infradiaphragmatic stasis-expelling decoction

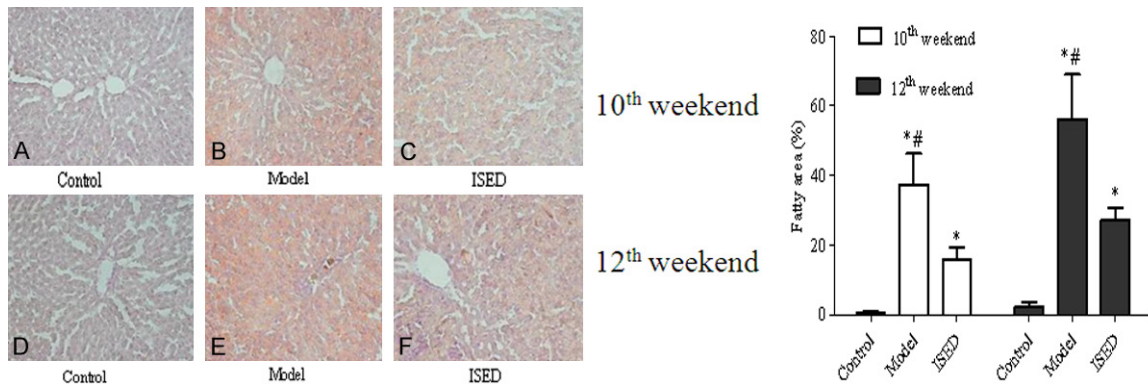


Figure 3. Adipocyte staining in livers. The orange indicated the fatty region. Twenty fields in a slide were randomly visualized under an Olympus IX-81 microscope (400×). The adipocyte cross-sectional area was calculated using an ImageJ 1.43 analyzing system. Blurry orange staining indicated a very low degree of steatosis in (A and D). Moderate orange staining indicated a middling degree of steatosis in (B and E). Lightly orange staining indicated a low degree of steatosis in (C and F). *P<0.05 vs Control, #P<0.05 vs ISED.

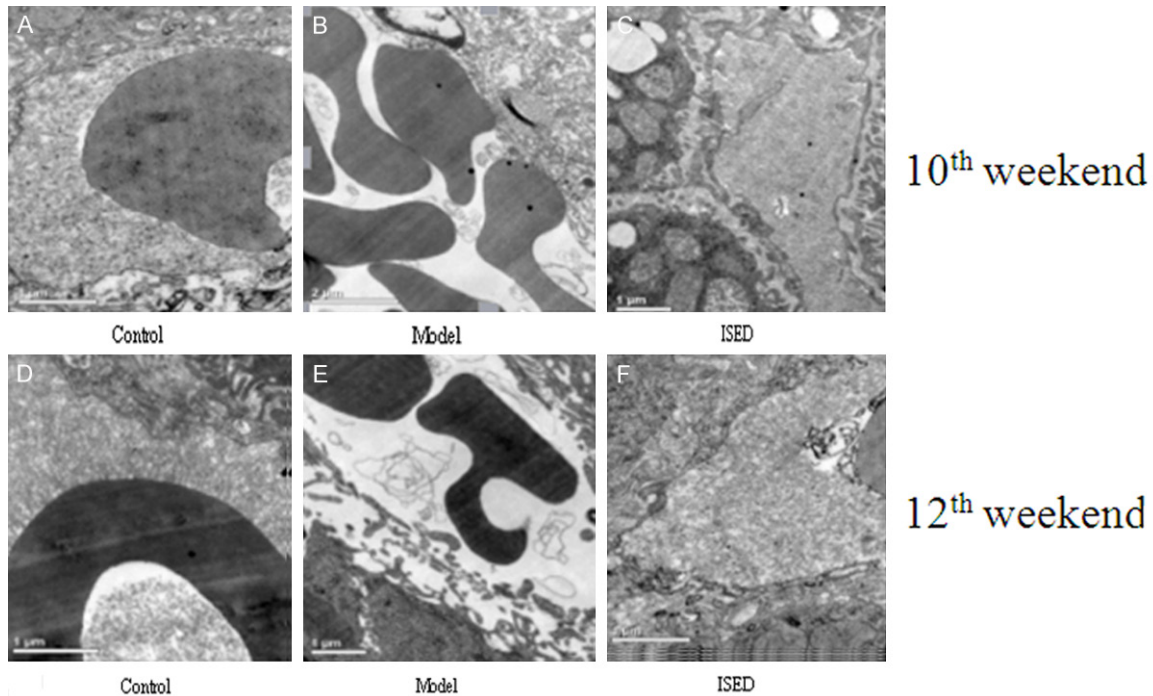


Figure 4. The ultrastructure of LSEC. LSEC was observed using a Philips CM 10 transmission electron microscope (12,000×). Approximately 30 sinusoids from each animal were assessed. The LSEC was sound in (A), (C), (D), and (F). LSEC was hurt and fragmentary. The mitochondria and endoplasmic reticulum of LSEC seemed inflatable in (B) and (E).

mentary in the model group during the whole treatment. The LSEC damage in the HFD-induced NAFLD rat model was ameliorated by ISED.

Discussion

Several studies have reported that a HFD can induce NAFLD [18, 19]. In a preliminary study,

we found that HFD induced the early symptoms of NAFLD in rats at the end of the 6th week by the measurement of ALT, TC, TG, et al. (data not shown). Therefore, gave an intragastrical administration of ISED to the rats at the beginning of the 9th week. Although the knowledge of the pathogenesis of NAFLD is limited, the increase of several parameters, such as BM, WLW, TC, TG, and HI were universally acknowl-

edged to be associated with the progression of NAFLD [20, 21]. During the whole experiment, the above parameters in the model group are all significantly higher than they were in the normal control group, indicating that the NAFLD model was superficially believable. The HE staining of liver tissues further confirmed that the HFD-induced NAFLD model was also pathologically reliable. After another 2 and 4 weeks ISED administration (at the end of the 10th and 12th weeks, respectively), it was found that the BM, WLW, TC, TG, and HI of rats in the ISED group were significantly lower than in the model group except the TC in serum, although the HFD was still fed to the animals in the duration. In the histopathological inspection, the structure of lobuli hepatis was normal and the hepatic cord was fitly arrayed at the end of the 10th and 12th weeks in the control group. However, a larger number of liver cells were turned into fatty cells, and the hepatic cord was irregular in the model group at the end of the 10th week. And a small percentage of liver cells was lightly steatotic in the ISED group at the end of the 10th week. By the end of the 12th week, almost all the liver cells were steatotic and swelling in the model group. The array of the hepatic cord in the ISED group at the end of the 12th week become more regular than it was at the end of the 10th week, but a small percentage of liver cells were still lightly steatotic. The Ultrastructure of LSEC was sound in the control and ISED groups at the end of both the 10th and 12th weeks. Comparatively, the LSEC in the model group was swollen during the period. Those biochemical and histopathological parameters consistently indicated that ISED can alleviate the NAFLD induced by HFD.

The levels of hypercoagulation and thrombophilia have been considered to be associated with the progress of NAFLD [22, 23]. Hypercoagulation and thrombophilia *in vitro* were generally represented by the parameters of hemorheology. The increase of PAR and WBF in hemorheology was the one of the indicators of the high levels of hypercoagulation and thrombophilia [24]. As predicted, the highest values of PAR and WBF were found in the model group, suggesting that the high levels of hypercoagulation and thrombophilia were possibly responsible for the NAFLD symptoms in rats. The above two parameters in the ISED group were significantly lower than those in the model group,

suggesting that the improvement of hypercoagulation and thrombophilia by ISED administration in the NAFLD rats. WBV consisted of LSV, MSV, and HSV, which was also associated with the number of red cells [25]. The abnormal increase of red cells indicated high levels of WBV, which were easily detected in patients with heart disease [26, 27]. Recently, the abnormal increase of red cell numbers was also revealed to be an important reason for the formation of hypercoagulation and thrombophilia in patients with hepatic fibrosis and liver cancer [28]. The analysis of LSV, MSV, and HSV showed that ISED decreases WBV in HFD-induced NAFLD rats by lowering LSV and MSV other than HSV. Furthermore, the red cells calculation demonstrated that the numbers of red cells in the control, model, and ISED groups were not significantly different. It was suggested that the decline of WBF by ISED administration in the NAFLD rats was not associated with an alternation in the numbers of red cells.

To further explore the possible mechanisms of ISED on the improvement of hypercoagulation and thrombophilia, the contents and m-RNA levels of the four cytokines relating to PAR were measured. Fib had the highest levels of clotting factor in serum, which was made of α , β , and γ chain [29]. Besides its participation in clotting, the combination of C-terminal of γ chain with the GPIIb/IIIa receptor was involved in the aggregation of pre-activated platelets [29]. It has been universally recognized that the high content and affinity of Fib with the GPIIb/IIIa receptor in serum was the stem factor for the hypercoagulation and thrombophilia in diabetes mellitus and metabolism syndrome [30, 31]. This hypothesis was also accepted by a group of researchers who focused on the investigation of liver illness associated with hypercoagulation and thrombophilia. The observed high levels of Fib and GPIIb/IIIa in the model group indicated that the two cytokines may contribute to the high levels of PAR, which in turn brought out the hypercoagulation and thrombophilia. A significant decline of Fib and GPIIb/IIIa contents in the ISED group compared to those in the model group suggested that the hypercoagulation and thrombophilia status in NAFLD rats was weakened by the ISED administration. CD62p was expressed in blood platelets in the progress of PAR [32]. When the blood platelets were activated, CD62p and vWF we-

re combined with Fib, thus causing hypercoagulation and thrombophilia [33]. High levels of CD62p and vWF were usually associated with CHD, AMI, and UAP [34]. The upregulation of CD62p and vWF were also reported in patients with fatty hepatitis, hepatic fibrosis, and liver cancer [35, 36]. In the current study, the CD62p and vWF levels in serum were both significantly lower in the ISED group relative to the model group. The decrease of PAR activity by ISED may be also associated with the decrease of CD62p and vWF.

A q RT-PCR showed that the m-RNA levels of Fib and CD62p in the ISED and control groups were at the same statistical levels, both of which were significantly lower than those in model group. Transcriptional regulation of ISED on Fib and CD62p m-RNA may be the reason for the decreased levels in the serum. However, the vWF and GPIIb/IIIa m-RNA levels in the ISED group were up-regulated and paralleled to the model group. Therefore, the post-translational regulation may be responsible for the decrease of vWF and the GPIIb/IIIa levels by the ISED administration in the NAFLD rats.

In conclusion, ISED can alleviate the symptoms of NAFLD. Two possible mechanisms are involved. The first is that ISED is capable of decreasing the TC, TG, ALT, and AST in serum and liver tissues. The second is to ameliorate the hypercoagulation and thrombophilia levels of NAFLD rats by decreasing the PAR and WBF, which is possibly associated with the reduction of vWF, GPIIb/IIIa, Fib, and CD62p contents in serum. The reasons for ISED-reduced vWF, GPIIb/IIIa, Fib, and CD62p contents occurred both at both the transcriptional and post-translational levels.

Acknowledgements

This work was supported by the National Natural Science Foundation of China [grant number 81260375].

Disclosure of conflict of interest

None.

Address correspondence to: Wenhui Chen, College of Pre-clinical Medicine, Yunnan University of Chinese Medicine, 1076# Yuhua Road, Kunming 650000, China. Tel: +86-871-6581908; E-mail: chenwenhui12@126.com

References

- [1] Ahmed MH and Byrne CD. Current treatment of non-alcoholic fatty liver disease. *Diabetes Obes Metab* 2010; 11: 188-195.
- [2] Siebler J and Galle PR. Treatment of nonalcoholic fatty liver disease. *World J Gastroenterol* 2006; 12: 2161-7.
- [3] Baffy G, Brunt EM and Caldwell SH. Hepatocellular carcinoma in non-alcoholic fatty liver disease: an emerging menace. *J Hepatol* 2012; 56: 1384-1391.
- [4] Baffy G. Hepatocellular carcinoma in non-alcoholic fatty liver disease: epidemiology, pathogenesis, and prevention. *J Clin Transl Hepatol* 2013; 1: 131-137.
- [5] Sookoian S and Pirola CJ. Non-alcoholic fatty liver disease is strongly associated with carotid atherosclerosis: a systematic review. *J Hepatol* 2008; 49: 600-607.
- [6] Preiss D and Sattar N. Non-alcoholic fatty liver disease: an overview of prevalence, diagnosis, pathogenesis and treatment considerations. *Clin Sci* 2008; 115: 141-150.
- [7] Powell EE, Jonsson JR and Clouston AD. Metabolic factors and non-alcoholic fatty liver disease as co-factors in other liver diseases. *Dig Dis* 2010; 28: 186-191.
- [8] Federico A, Zulli C, De SI, Del PA, Dallio M, Masarone M and Loguercio C. Focus on emerging drugs for the treatment of patients with non-alcoholic fatty liver disease. *World J Gastroenterol* 2014; 20: 16841-16857.
- [9] Sun Q. Chinese and Western medicine treatment of non-alcoholic fatty liver disease. *J Pract Tradit Chin Int Med* 2013; 28: 427-433.
- [10] Hirotsani Y, Doi A, Takahashi T, Umezawa H, Urashima Y and Myotoku M. Protective effects of the herbal medicine goshajinkigan in a rat model of non-alcoholic fatty liver disease. *Biomed Res* 2012; 33: 373.
- [11] Liu T, Tang ZP and Ji G. Treatment of non-alcoholic fatty liver disease based on traditional Chinese medicine therapies for warming yang to activate qi. *Zhong Xi Yi Jie He Xue Bao* 2011; 9: 135-137.
- [12] Fan JG and Farrell GC. Epidemiology of non-alcoholic fatty liver disease in China. *J Hepatol* 2009; 50: 204-210.
- [13] Cheng JT. Review: drug therapy in Chinese traditional medicine. *J Clin Pharmacol* 2000; 40: 445-450.
- [14] Li Z. The clinical curative effect of Infradiaphragmatic Stasis-Expelling Decoction in the treatment of endometriosis with infertility. *Guid China Med* 2014; 45: 178-179.
- [15] Xueru MA; Gastroenterology DO. Application of infradiaphragmatic Stasis-Expelling Decoction plus lamivudine in treatment of hepatitis B liv-

Infradiaphragmatic stasis-expelling decoction

- er cirrhosis. *China Mod Doc* 2016; 12: 122-124.
- [16] Lu CX, Wu HK and Wu SS. Exploration of prestigious chinese doctor Wu Shoushan's law of drug use in the treatment of hepatocirrhosis based on data mining. *Henan Tradit Chin Med* 2017; 12: 15-17.
- [17] Wang JJ, Xia JL, Guo Q, Tian Y, Zhang Y, Wang YG, Wang L; Pharmacy DO. Influence of Infradiaphragmatic Stasis-Expelling Decoction combined with octreotide, thrombin on liver function and serum NO and ACE of patients with cirrhosis complicated with gastroesophageal varices blood. *Chin J Integrated Tradit & Western Med* 2017; 12: 55-59.
- [18] Castro GS, Cardoso JF, Vannucchi H, Zucoloto S and Jordao AA. Fructose and NAFLD: metabolic implications and models of induction in rats. *Acta Cir Bras* 2011; 26 Suppl 2: 45-50.
- [19] Liang W, Menke AL, Driessen A, Koek GH, Lindeman JH, Stoop R, Havekes LM, Kleemann R and van den Hoek AM. Establishment of a general NAFLD scoring system for rodent models and comparison to human liver pathology. *PLoS One* 2014; 9: e115922.
- [20] Loomba R and Chalasani N. The hierarchical model of NAFLD: prognostic significance of histologic features in NASH. *Gastroenterology* 2015; 149: 278-281.
- [21] Shridhar N, Vijayaraj D, Nagaraj MK, Pranisha S, Jaji MS, Rajesh BN and Jeyamurugan M. Effect of BLX-1002 on key features of non alcoholic fatty liver disease (NAFLD) in animal models. *Diabetes* 2011; 60: 288-289.
- [22] Iyer S, Upadhyay PK, Majumdar SS and Nagarajan P. Animal models correlating immune cells for the development of NAFLD/NASH. *J Clin Exp Hepatol* 2015; 5: 239-245.
- [23] Northup PG, Sundaram V, Fallon MB, Reddy KR, Balogun RA, Sanyal AJ, Anstee QM, Hoffman MR, Ikura Y, Caldwell SH; Coagulation in Liver Disease G. Hypercoagulation and thrombophilia in liver disease. *J Thromb Haemost* 2008; 6: 2-9.
- [24] Targher G, Chonchol M, Miele L, Zoppini G, Picchiri I and Muggeo M. Nonalcoholic fatty liver disease as a contributor to hypercoagulation and thrombophilia in the metabolic syndrome. *Semin Thromb Hemost* 2009; 35: 277-287.
- [25] Irace C, Scarinci F, Scorcia V, Bruzzichessi D, Fiorentino R, Randazzo G, Scorcia G and Gnasso A. Association among low whole blood viscosity, haematocrit, haemoglobin and diabetic retinopathy in subjects with type 2 diabetes. *Br J Ophthalmol* 2011; 95: 94.
- [26] Canaud B, Rodriguez A, Chenine L, Morena M, Jaussent I, Leray-Moragues H, Picardl A and Cristo JP. Whole-blood viscosity increases significantly in small arteries and capillaries in hemodiafiltration. Does acute hemorheological change trigger cardiovascular risk events in hemodialysis patient? *Hemodial Int* 2010; 14: 433-440.
- [27] De Backer TL, De Buyzere M, Segers P, Carlier S, Sutter JD, Van de Wiere C and De Backer G. The role of whole blood viscosity in premature coronary artery disease in women. *Atherosclerosis* 2002; 165: 367-373.
- [28] Kim HM, Kim BS, Cho KY, Kim BI, Sohn CI, Jeon WK, Kim HJ, Park DI and Park JH. Elevated red cell distribution width is associated with advanced fibrosis in NAFLD. *Clin Mol Hepatol* 2013; 19: 258-265.
- [29] Mosesson MW. Fibrinogen and fibrin structure and functions. *J Thromb Haemost* 2010; 3: 1894-1904.
- [30] Yang J, Li S and Liu YX. Systematic analysis of diabetes- and glucose metabolism-related proteins and its application to Alzheimer's disease. *J Biomed Sci Eng* 2013; 06: 615-644.
- [31] Razmara M, Hjemdahl P, Ostenson CG and Li N. Platelet hyperprocoagulant activity in type 2 diabetes mellitus: attenuation by glycoprotein IIb/IIIa inhibition. *J Thromb Haemost* 2008; 6: 2186-2192.
- [32] Choudhury A, Chung I, Blann AD and Lip GY. Platelet surface CD62P and CD63, mean platelet volume, and soluble/platelet P-selectin as indexes of platelet function in atrial fibrillation: a comparison of "healthy control subjects" and "disease control subjects" in sinus rhythm. *J Am Coll Cardiol* 2007; 49: 1957-1964.
- [33] Zeng ZY, Ouyang LL, Ming-Fen LI and Huang XQ. Clinical significance of plasma levels of CD62P, CD63, vWF and vWF-cp in patients with type 2 diabetes mellitus and coronary artery disease. *Int Med China* 2009.
- [34] Su Z, Du J and Wenqing C. The significance on examination of CD62P, CD63 and vWF in patients with acute myocardial infarction or atrial fibrillation. *Pract J Card Cerebral Pneumal & Vas Dis* 2004.
- [35] McPherson S, Hardy T, Henderson E, Burt AD, Day CP and Anstee QM. Evidence of NAFLD progression from steatosis to fibrosing-steatohepatitis using paired biopsies: implications for prognosis and clinical management. *J Hepatol* 2015; 62: 1148-1155.
- [36] Kotronen A, Joutsu-Korhonen L, Sevastianova K, Bergholm R, Hakkarainen A, Pietiläinen KH, Lundbom N, Rissanen A, Lassila R and Yki-Jarvinen H. Increased coagulation factor VIII, IX, XI and XII activities in non-alcoholic fatty liver disease. *Liver Int* 2011; 31: 176-183.